Thermal conductivity of semicrystalline polymers – a model

C. L. Choy and K. Young
Department of Physics, The Chinese University of Hong Kong, Hong Kong
(Received 13 December 1976; revised 4 Febraury 1977)

The thermal conductivity of semicrystalline polymers, regarded as two-phase materials, is discussed in terms of the Maxwell model generalized to the case where the inclusions are thermally anisotropic. The predicted effect of orientation agrees well with the large anisotropy observed in oriented polymers. The conductivity of the crystallites normal to the chain axes has also been extracted using this model. A recently proposed model for composites which incorporates interfacial boundary resistance has been applied to the low temperature data for poly(ethylene terephthalate), not only explaining the decrease of conductivity with crystallinity, but also allowing the effective crystallite shape and the boundary resistance to be determined. The latter is found to vary as T^{-2}.

INTRODUCTION

Two interesting features of the thermal conductivity of semicrystalline polymers have recently been observed[1–4]. First, while the thermal conductivity increases with crystallinity at high temperature, it exhibits the opposite trend[1] below about 20K. Secondly, at high temperature, orientation has a large effect which diminishes rapidly as the temperature is reduced[2–4]. Physically, the high temperature behaviour can be easily understood if we recognize the fact that the thermal conductivity of the crystallites along the chain direction is much higher than the value in the perpendicular direction which, in turn, is comparable to the thermal conductivity of the amorphous region. On the other hand, the thermal resistance at low temperature is dominated by the boundary resistance at amorphous–crystalline interfaces, which gives rise to a reduction in thermal conductivity with increasing interface area (i.e. with crystallinity) and relative insensitivity to orientation.

On the basis of these ideas crude models have been proposed and found to give results in reasonable agreement with experiment[1–3]. In the present study we consider a slightly more refined model which, among other predictions, will explain the change of conductivity both along and normal to the orientation direction as a function of the degree of orientation. The orientation of the chain axis of the crystallities is normally characterized by an orientation function f_c which, for most polymers, has already been determined as a function of draw (or extrusion) ratio from wide-angle X-ray diffraction, thus facilitating our analysis.

In the next two sections the model will be discussed in detail and then applied to a variety of isotropic and oriented polymer samples. In the final section we will indicate the role of interface boundary resistance and its effect on the low temperature behaviour.

THE MODEL

Our model for semicrystalline polymers consists of axially symmetric crystallites embedded in an amorphous medium and occupying a volume fraction X. We first limit our discussion to high temperatures ($T \geqslant 70$K) where the effect of boundary resistance may be neglected. There is evidence that, for draw ratios not too large (say up to 4), the conductivity of the amorphous phase remains approximately unchanged[5,6], so we describe the amorphous phase by an isotropic conductivity K_a. The crystalline phase is, however, intrinsically anisotropic and must be characterized by conductivities $K_{c\parallel}$ and $K_{c\perp}$ in directions parallel and perpendicular to the chain axis. Since the intrachain covalent bond is much stronger than the interchain Van der Waals interaction, conductivity along the chains is expected to be large, while that perpendicular to the chains should not differ substantially from the amorphous case, i.e.

$$k_{\parallel} \equiv \frac{K_{c\parallel}}{K_a} \gg 1 \qquad k_{\perp} \equiv \frac{K_{c\perp}}{K_a} \simeq 1 \qquad (1)$$

For an undrawn polymer, the distribution of c-axes is random, but after drawing, the angle θ between the c-axes and the draw direction shifts to smaller values, this being characterized by the orientation function f_c given by:

$$f_c = \tfrac{1}{2}[3\langle\cos^2\theta\rangle - 1] \qquad 0 \leqslant f_c \leqslant 1 \qquad (2)$$

where $\langle\,\rangle$ denotes the average over all crystallites. It is clear that the very large intrinsic anistropy of the crystalline phase, together with the possibility of orienting the c-axes close to the draw direction, is responsible for the large anistropy observed. To have any chance of success, the model must treat these effects realistically.

One might also expect the shape of the crystallites to be an important parameter. However, it is rather unclear what shape factor to assign to the crystallites. Although it is generally agreed that the basic crystalline units are plate-like lamellae with lateral dimensions much larger than thickness[7] there is also considerable evidence that the lamellae are in turn composed of mosaic blocks of lateral dimensions 100–300 Å (which is comparable to their thickness), with boundaries defined by dislocations[8–11]. Moreover, the interlamellar amorphous regions and the intermosaic block regions have been termed the amorphous state of the first and second kind, respectively[12], so a semicrystalline speci-

men is, strictly speaking, a three-phase composite. However, at high temperatures where boundary resistance is negligible these two kinds of amorphous region can be treated as identical as a first approximation, so a semicrystalline polymer will be considered as a two-phase material with spherical crystalline inclusions.

In the development of the model, it will be convenient to use the dielectric analogue in order to be able to invoke familiar concepts such as polarizability and surface charge densities. Thus the amorphous phase is taken as a medium with unit dielectric constant ($D_i = \delta_{ij}E_j$) while each crystallite is a sphere with a dielectric constant ϵ_{ij}($D_i = \epsilon_{ij}E_j$). There are two reference frames to be considered: a frame S defined by the draw direction, and (for each crystallite) a frame S' defined by its c-axis. In the latter frame ϵ'_{ij} takes the diagonal form:

$$\epsilon'_{ij} = \text{diag}\ (\epsilon'_{xx}, \epsilon'_{xx}, \epsilon'_{zz})$$

The crucial question is the interaction of one sphere with another. The simplest approach is to treat this in an average manner. We focus attention on one sphere, which we take to be at the origin of the coordinate system, and construct around it a spherical cavity enclosing no other crystalline sphere. The region outside the cavity will be treated macroscopically as a medium with a dielectric tensor $\bar{\epsilon}_{ij}$ which corresponds to the dielectric constant of the composite as a whole and is in fact the object to be determined. In the frame S, $\bar{\epsilon}_{ij}$ takes the diagonal form:

$$\bar{\epsilon}_{ij} = \text{diag}\ (\bar{\epsilon}_{xx}, \bar{\epsilon}_{xx}, \bar{\epsilon}_{zz})$$

Imagine an average field $\vec{E}$ in the macroscopic medium outside the cavity. The field $\vec{F}$ inside the cavity will have an extra contribution from the surface charge σ on the walls of the cavity arising from the polarization $\vec{P}$:

$$\vec{F} = \vec{E} - \int \frac{\sigma(\vec{r})\vec{r}}{r^3}\,\mathrm{d}S \tag{3}$$

where $\sigma = -\vec{P}\cdot\vec{n}$ and $\vec{n} = \vec{r}/r$. So:

$$\begin{aligned}\sigma &= -n_i P_i \\ &= -\frac{1}{4\pi} n_i (D_i - E_i) \\ &= -\frac{1}{4\pi} n_i (\bar{\epsilon}_{ij} - \delta_{ij}) E_j\end{aligned}$$

Putting this into equation (3) we find:

$$\begin{aligned}F_i &= Z_{ij}E_j \\ &= [\delta_{ij} + \frac{1}{3}(\bar{\epsilon}_{ij} - \delta_{ij})]E_j\end{aligned} \tag{4}$$

The cavity field factor Z_{ij} is diagonal in the S frame:

$$Z_{xx} = F_x/E_x = F_y/E_y = \frac{\bar{\epsilon}_{xx} + 2}{3} \tag{5a}$$

$$Z_{zz} = F_z/E_z = \frac{\bar{\epsilon}_{zz} + 2}{3} \tag{5b}$$

It is this field $\vec{F}$ which induces a dipole moment $\vec{p}$ on each sphere. The calculation of $\vec{p}$ is standard and the result may be expressed in terms of a polarizability tensor α_{ij}:

$$p_i = \alpha_{ij}F_j \tag{6}$$

where the polarizability tensor is diagonal in the S' frame:

$$\alpha'_{ij} = \text{diag}\left(a^3\frac{\epsilon'_{xx} - 1}{\epsilon'_{xx} + 2}, a^3\frac{\epsilon'_{xx} - 1}{\epsilon'_{xx} + 2}, a^3\frac{\epsilon'_{zz} - 1}{\epsilon'_{zz} + 2}\right) \tag{7}$$

Here a is the radius of the sphere.

Now the displacement vector D is :

$$\begin{aligned}D_i &= E_i + 4\pi P_i \\ &= [\delta_{ij} + 4\pi N\langle\alpha_{ij}\rangle]\,F_j \\ &= [\delta_{ij} + 4\pi N\langle\alpha_{ij}\rangle]\,Z_{jk}E_k\end{aligned} \tag{8}$$

where $N = 3X/4\pi a^3$ is the number of spheres per unit volume and $\langle\ \rangle$ denotes average. This allows us to identify the macroscopic dielectric constant $\bar{\epsilon}_{ij}$ as:

$$\bar{\epsilon}_{ik} = [\delta_{ij} + 4\pi N\langle\alpha_{ij}\rangle]\,Z_{jk} \tag{9}$$

Now α_{ij} is related to α'_{ij} by a coordinate rotation and it is easy to show that:

$$\langle\alpha_{xx}\rangle = \langle\alpha_{yy}\rangle = \tfrac{1}{2}(1 + \langle\cos^2\theta\rangle)\alpha'_{xx} + \tfrac{1}{2}\langle\sin^2\theta\rangle\alpha'_{zz} \tag{10a}$$

$$\langle\alpha_{zz}\rangle = \langle\sin^2\theta\rangle\ \alpha'_{xx} + \langle\cos^2\theta\rangle\alpha'_{zz} \tag{10b}$$

Putting these together we find:

$$\bar{\epsilon}_{zz} - 1 = 3X\left[\frac{\epsilon'_{xx} - 1}{\epsilon'_{xx} + 2}\langle\sin^2\theta\rangle + \frac{\epsilon'_{zz} - 1}{\epsilon'_{zz} + 2}\langle\cos^2\theta\rangle\right]\frac{\bar{\epsilon}_{zz} + 2}{3} \tag{11}$$

and analogously for the transverse directions. To go back to thermal conductivities, we simply transcribe according to $\epsilon'_{xx} \to k_\perp$, $\epsilon'_{zz} \to k_\parallel$, $\bar{\epsilon}_{xx} \to K_\perp/K_a$, $\bar{\epsilon}_{zz} \to K_\parallel/K_a$ and therefore obtain:

$$\frac{K_\perp - K_a}{K_\perp + 2K_a} = X\left[\frac{k_\perp - 1}{k_\perp + 2}\ \ \frac{1 + \langle\cos^2\theta\rangle}{2} + \frac{k_\parallel - 1}{k_\parallel + 2}\,\tfrac{1}{2}\langle\sin^2\theta\rangle\right] \tag{12a}$$

$$\frac{K_\parallel - K_a}{K_\parallel + 2K_a} = X\left[\frac{k_\perp - 1}{k_\perp + 2}\langle\sin^2\theta\rangle + \frac{k_\parallel - 1}{k_\parallel + 2}\langle\cos^2\theta\rangle\right] \tag{12b}$$

For complete orientation ($\langle\cos^2\theta\rangle = 1$), $K_\perp(K_\parallel)$, depends only on $K_{c\perp}(K_{c\parallel})$, as expected. On the other hand, in the absence of orientation, the isotropic conductivity K_i can be obtained by putting $\langle\cos^2\theta\rangle = 1/3$ in either equation (12a) and (12b), and is

$$\frac{K_i - K_a}{K_i + 2K_a} = X\left[\frac{2}{3}\frac{k_\perp - 1}{k_\perp + 2} + \frac{1}{3}\frac{k_\parallel - 1}{k_\parallel + 2}\right] \tag{13}$$

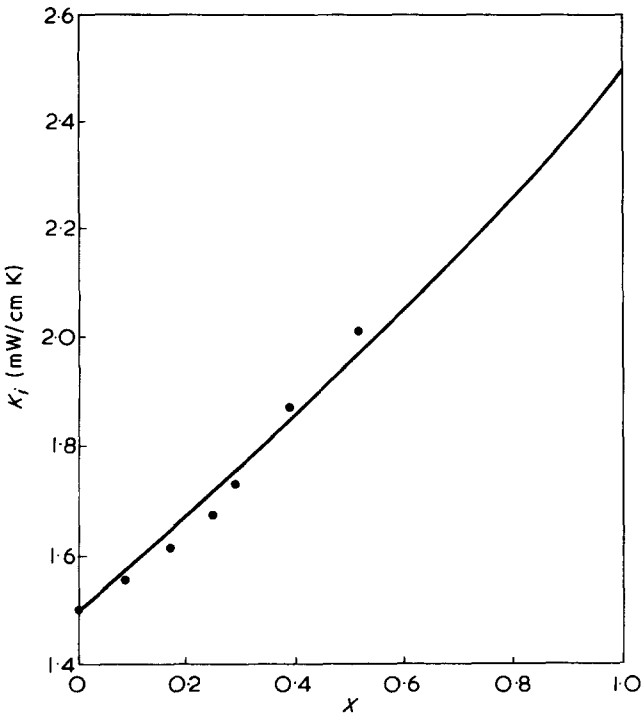

Figure 1 The crystallinity dependence of the thermal conductivity of isotropic PET at 70K. ●, data from ref 1; ——, calculated according to equation (13)

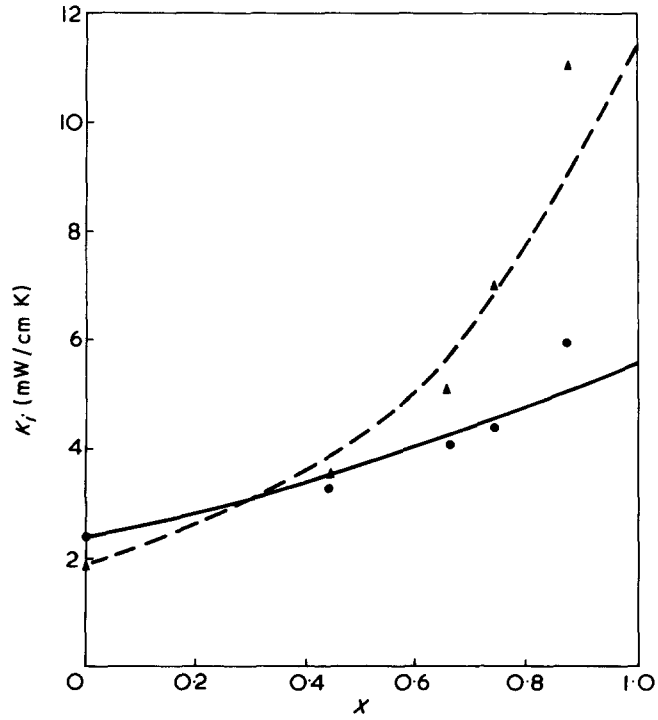

Figure 2 The crystallinity dependence of the thermal conductivity of isotropic PE at 100 and 300K. 300K: data (●); theoretical (——) 100K: data (▲), theoretical (— — — —). The curves are calculated according to equation (13). Data from ref 17

We have previously mentioned that on physical grounds $k_{//} \gg 1$, so that $(k_{//} - 1)/(k_{//} + 2) \simeq 1$; hence equations (12) and (13) are almost independent of the actual value of $k_{//}$. Thus it will not be possible to determine the magnitude or temperature dependenee of $K_{c//}$ from experimental data.

From the above derivation it is seen that the average treatment of other spheres closely parallels that of the Maxwell model[13]. Indeed, in the special case where the crystalline phase is isotropic ($k_{//} = k_{\perp}$), our results reduce to the well-known Maxwell expression[13]. There are of course more sophisticated and accurate treatments of the interaction among spheres in the isotropic case[14–16], but in the present context there are so many other relevant factors – the intrinsic anisotropy and orientation of the crystallites, for example – that a detailed consideration of the interaction does not appear to be worthwhile at this stage.

COMPARISON WITH EXPERIMENTS

Conductivity of isotropic polymers

With the assumption of $(k_{//} - 1)/(k_{//} + 2) \simeq 1$ and known value of K_a, it follows from equation (13) that K_i depends only on $K_{c\perp}$. *Figures 1* and *2* show the fitting of the experimental data for poly(ethylene terephthalate) (PET)[1] and polyethylene (PE)[17] to equation (13). It is clear that a good fit is obtained. The resulting $K_{c\perp}$ values for these two polymers, as well as that for polypropylene (PP), are shown against temperature in *Figure 3*.

It is clearly seen that $K_{c\perp}$ of PE is much larger than those for the other two polymers and follows approximately a T^{-1}

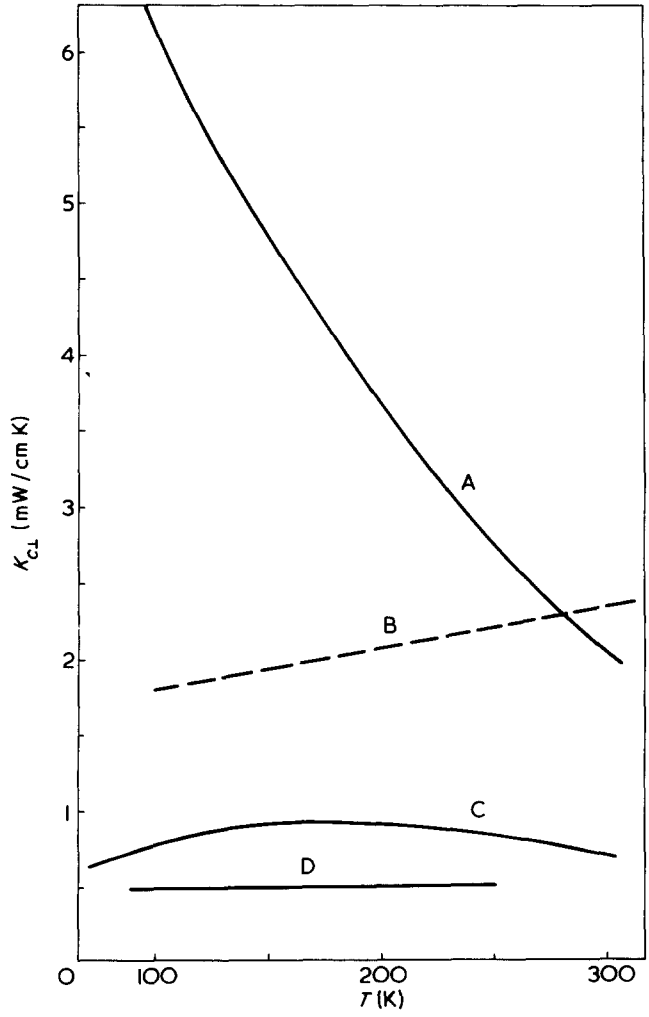

Figure 3 The temperature dependence of the thermal conductivity of the crystallites normal to the chain axis for PE, PET and PP. For comparison we also show K_a, which is the thermal conductivity of amorphous PE obtained by extrapolation of the data for the melt[37]. Its value is typical of *all* amorphous polymers. A, PE; B, K_a; C, PET; D, PP

Table 1 Comparison of the theoretically predicted thermal conductivity K_i, $K_{i,s}$ and $K_{i,p}$ with the observed values K_i (expt) for isotropic polymer samples

Material	K_a	λ	$K_{/\!/}$	$K_\perp$	K_i	$K_{i,s}$	$K_{i,p}$	K_i (expt)
PET[a] 100K $X \approx 0.42$	1.8	3.6	3.9	2.0	2.22	2.39	2.63	2.2
PP[a] 100K $X \approx 0.62$	1.35[b]	3.3	3.2	1.5	1.95	1.82	2.07	1.75
		5.5	5.2	1.3	2.09	1.73	2.60	1.75
PP[a] 100K $X \approx 0.79$	1.35[b]	10.5	7.8	1.2	2.23	1.67	3.40	1.91
PE[c] 323K $X \approx 0.69$	2.4[d]	1.64	8.86	4.18	5.34	5.07	5.74	4.89
		3.3	16.5	3.2	5.30	4.38	7.63	
		4.03	23.4	2.9	5.36	4.10	9.73	
		5.14	30.3	2.72	5.39	3.90	11.91	
		9.26	40.6	2.3	5.08	3.35	15.07	
		13.8	42.1	2.1	4.84	3.07	15.43	
PE[e] 100K $X = 0.6$	1.8[d]	4.4	21	4.4	6.72	5.97	9.93	7.4
PE[f] 100K $X = 0.78$	1.8[d]	5.4	31.5	5.3	8.25	7.33	14.03	10
		9.5	42	5.3	8.56	7.48	17.53	
		13	52	5.3	8.76	7.56	20.87	

[a] Data from ref 3; [b] K_a is obtained from ref 17; [c] Data from ref 27; [d] K_a is obtained by extrapolation of the data for the melt given in ref 37; [e] Data from ref 2; [f] Data from ref 4

dependence, which is characteristic of three-phonon Umklapp scattering processes[18]. Moreover, not only this dependence but also the magnitude are about the same as the conductivity of molecular crystals such as benzene (C_6H_6)[19], which probably possesses a Van der Waals interaction of similar strength. We also note that, while at 100K $K_{c\perp}$ is more than three times larger than K_a, these two quantities have roughly the same values at room temperature as a result of the vastly different temperature dependence. The values of $K_{c\perp}$ of the other two polymers are even lower than K_a, and almost independent of temperature within the accuracy of our analysis. While these low values may arise from weaker interchain Van der Waals interaction, the only possible explanation for the gentle temperature dependence seems to be phonon scattering by defects in the crystallites.

Eiermann[17] has performed similar analysis employing the Maxwell model. But since the Maxwell model applies only to two isotropic phases, he was forced to describe the crystalline phase with an effective isotropic conductivity K_c^{eff}, which must be some average measure of the more physical $K_{c/\!/}$ and $K_{c\perp}$ used in our analysis. In fact, by comparing the Maxwell model:

$$\frac{K_i - K_a}{K_i + 2K_a} = X \frac{K_c^{\text{eff}} - K_a}{K_c^{\text{eff}} + 2K_a}$$

with equation (13), it is seen that Eiermann's K_c^{eff} is related to our $K_{c/\!/}$ and $K_{c\perp}$ as:

$$\frac{K_c^{\text{eff}} - K_a}{K_c^{\text{eff}} + 2K_a} = \frac{2}{3}\frac{K_{c\perp} - K_a}{K_{c\perp} + 2K_a} + \frac{1}{3}\frac{K_{c/\!/} - K_a}{K_{c/\!/} + 2K_a}$$

$$\simeq \frac{2}{3}\frac{K_{c\perp} - K_a}{K_{c\perp} + 2K_a} + \frac{1}{3} \qquad (14)$$

Because $K_{c/\!/}$ and $K_{c\perp}$ differ so much, their average as represented by K_c^{eff} has no real physical significance.

A test of the model

Without having to know the orientation function f_c or the crystallinity X, our model gives a relation between the conductivities $K_{/\!/}$ and $K_\perp$ of the drawn polymer and the isotropic conductivity K_i before drawing. If the isotropic and drawn samples have the same crystallinity this relation can be readily obtained from (12) and reads:

$$\frac{K_i - K_a}{K_i + 2K_a} = \frac{1}{3}\frac{K_{/\!/} - K_a}{K_{/\!/} + 2K_a} + \frac{2}{3}\frac{K_\perp - K_a}{K_\perp + 2K_a} \qquad (15)$$

This can be used with the data on $K_{/\!/}$ and $K_\perp$ at each draw ratio to predict K_i, the accuracy of this prediction then being a parameter-free test of the model.

It is instructive to compare this with the aggregate model [20–24] which also predicts K_i from a knowledge of $K_{/\!/}$ and $K_\perp$. However, the aggregate model suffers from a number of drawbacks when applied to semicrystalline polymers. First, it considers the sample as a single phase which, especially for polymers with comparatively high crystallinity, appears to be unrealistic. Moreover, since the sample contains both crystalline and amorphous regions, it is not clear whether the orientation function in such one-phase models should be related to the crystalline orientation function f_c or the amorphous orientation function f_a. Furthermore, one-phase models are also unsuitable for the discussion of crystallinity dependence and, in particular, the interplay between orientation and crystallinity. Another critical problem is that, in performing the average over the aggregate, there is no reason to prefer either averaging the resistivities (the series model) or the conductivities (the parallel model). If we denote the predicted value of K_i by these two methods by $K_{i,s}$ and $K_{i,p}$ respectively, then:

$$K_{i,s}^{-1} = \frac{1}{3}K_{/\!/}^{-1} + \frac{2}{3}K_\perp^{-1} \qquad (16)$$

$$K_{i,p} = \frac{1}{3}K_{/\!/} + \frac{2}{3}K_\perp \qquad (17)$$

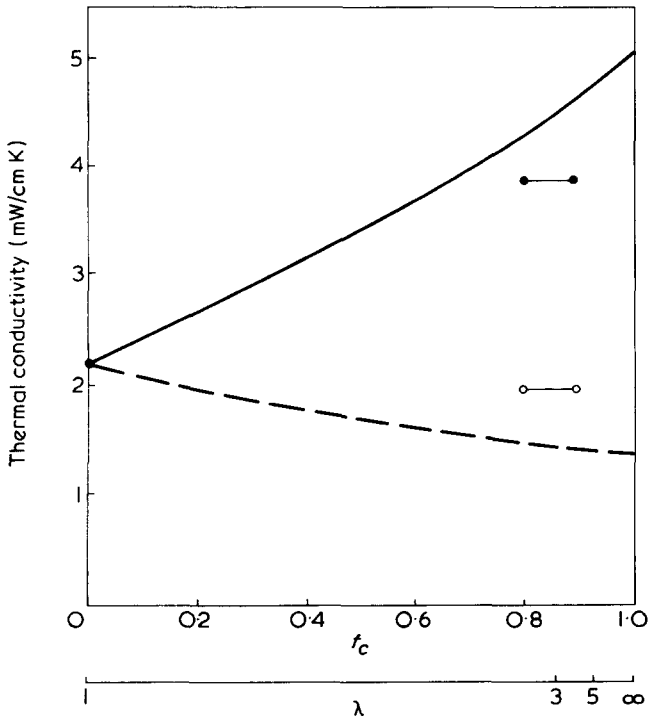

Figure 4 The thermal conductivity of extruded PET at 100K against the crystalline orientation function. Data from ref 3: ●, $K_{//}$; ○, $K_{\perp}$. The horizontal error bar is due to the uncertainty in f_c as explained in the text. The theoretical curves for $K_{//}$ (———) and $K_{\perp}$ (– – – –) are calculated according to equation (19)

In general one can only expect $K_{i,s}$ and $K_{i,p}$ to bound the true K_i, so that the constraint is not at all stringent. It may be mentioned that the same problem besets the application of the aggregate model to the elastic moduli of oriented polymers[25,26].

In *Table 1* we list the predicted values K_i, $K_{i,s}$ and $K_{i,p}$ for PET, PP and PE. The experimental values are, in general, within 10% of our predicted K_i, while the agreement with $K_{i,s}$ and $K_{i,p}$ (especially the latter) is much worse. For PP, the value of $K_{\perp}$ is only available[3] for extrusion ratio $\lambda = 10.5$, but because of its weak dependence on λ, the values for other extrusion ratios can be obtained by interpolation.

The fact that $K_{i,s}$ agrees better with data than $K_{i,p}$ follows naturally from our model, since normally $K_a < K_i, K_{//}, K_{\perp}$, so if we expand equation (15) to the lowest non-trivial order in K_a, it reduces to the 'series' expression

$$K_i^{-1} = \frac{1}{3}K_{//}^{-1} + \frac{2}{3}K_i^{-1} \tag{18}$$

Conductivity as a function of orientation

The dependence of $K_{//}$ and $K_{\perp}$ on the orientation parameter f_c is predicted by equation (12), which for this purpose may be written as:

$$K_{\perp,//} = K_a \cdot \frac{1 + 2XQ_{\perp,//}}{1 - XQ_{\perp,//}} \tag{19}$$

where, assuming $(k_{//} - 1)/(k_{//} + 2) \simeq 1$:

$$Q_{\perp} = \frac{1}{3}\left(2\frac{k_{\perp} - 1}{k_{\perp} + 2}\right) + 1 \quad -\frac{1}{3}\left(1 - \frac{k_{\perp} - 1}{k_{\perp} + 2}\right)f_c$$

$$Q_{//} = \frac{1}{3}\left(2\frac{k_{\perp} - 1}{k_{\perp} + 2} + 1\right) + \frac{1}{3}\left(1 - \frac{k_{\perp} - 1}{k_{\perp} + 2}\right)2f_c \tag{20b}$$

Since $k_{\perp}$ has already been determined from the isotropic data, there are no adjustable parameters in equation (19). The predicted behaviour as a function of f_c is shown in *Figures 4* to *6*, together with the experimental data. In each case, the value of f_c for a given draw ratio has been obtained from the literature[28–31]. For PET and PE, the samples used for X-ray determination of f_c were not the same as those for thermal measurements[3,27], thus causing an uncertainty in the value of f_c, represented by horizontal error bars. For PP, the data point at $\lambda = 10.5$ ($f_c \simeq 1$) corresponds to a sample whose crystallinity increases appreciably on extrusion to $X = 0.79$, while the other data points refer to $X = 0.62$; hence two theoretical curves have been drawn.

It is clear that our model is in fair agreement with experiment and certainly gives the right trends: $K_{//}$ increases rapidly with f_c, while $K_{\perp}$ shows a slight decrease. For PE, the experimental value of $K_{//}$ show a sudden sharp rise at draw ratio larger than 4 ($f_c > 0.9$), which we take to be an indication that effects other than crystalline orientation (as described by f_c) begin to be important. This is consistent with earlier studies[4] which show that this further rise can be explained

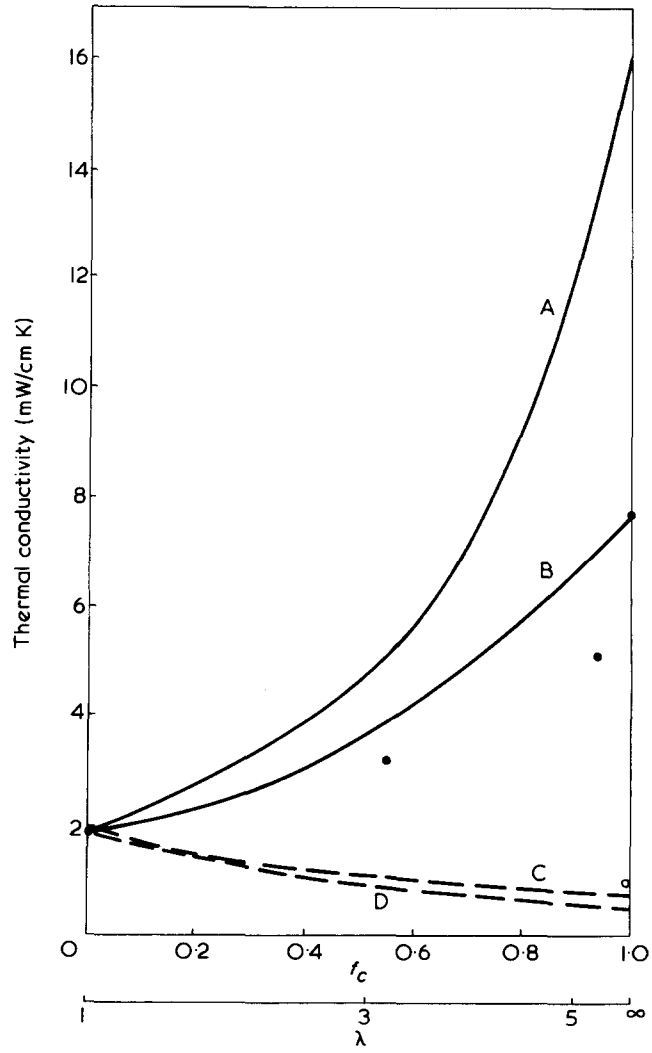

Figure 5 The thermal conductivity of extruded PP at 100K against the crystalline orientation function. The legends are given in the caption to *Figure 4*. A, $X = 0.79$; B, $X = 0.62$; C, $X = 0.62$; D, $X = 0.79$

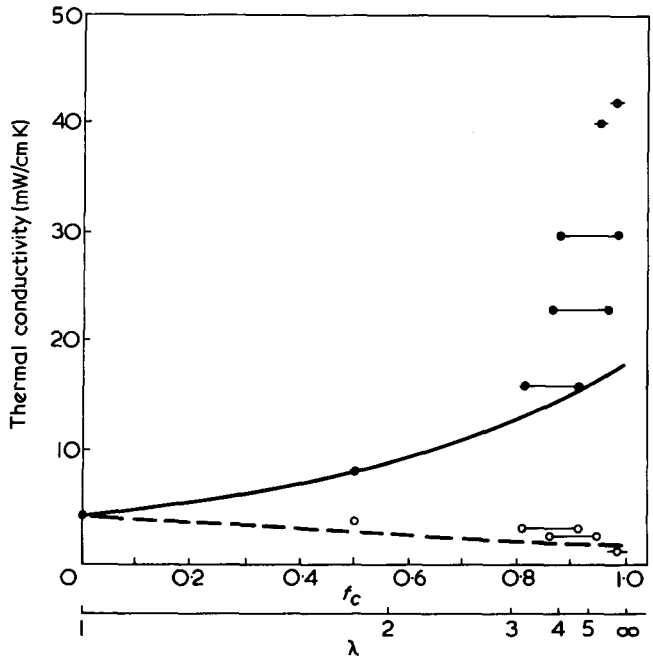

Figure 6 The thermal conductivity of oriented PE at 323K against the crystalline orientation function. The legends are given in the caption to *Figure 4*. Data from ref 27

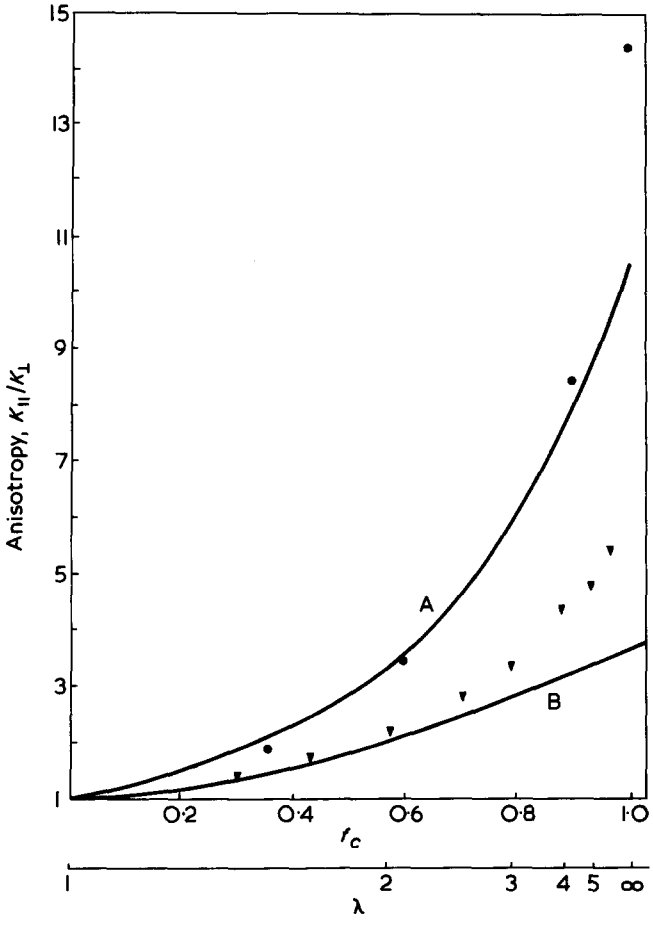

Figure 7 The anisotropy in the thermal conductivity of drawn PE at room temperature against the crystalline orientation function. A, $X = 0.74$; B, $X = 0.45$. The theoretical curves are calculated according to equation (19). Data from ref 24

by taking into account the effect of tie molecules forming intercrystalline bridges. Since these taut tie molecules are oriented along the draw direction they have little effect on $K_{\perp}$, so our prediction of $K_{\perp}$ is valid for large draw ratios, and this is borne out by the data.

For PE, the anisotropy $A = K_{\parallel}/K_{\perp}$ has also been measured[24] as a function of draw ratio for two samples with vastly different crystallinities ($X = 0.45, 0.74$), the result clearly demonstrating the interplay between orientation and crystallinity (*Figure 7*). The most important feature, namely that the anisotropy A increases more rapidly with f_c for larger crystallinities X, is adequately reproduced by our model, and quantitative agreement is satisfactory for $\lambda < 4$, as shown by the theoretical curves. The discrepancy for larger λ is due to the effect of tie molecules on $K_{\parallel}$, as previously discussed. The observed anisotropy has also been explained in terms of an aggregate model where the intrinsic anistropy of the basic units is assumed to be crystallinity-dependent[24]. However, in view of the large difference in K_a and $K_{c\parallel}$, our treatment seems more realistic.

LOW TEMPERATURE BEHAVIOUR

In addition to the effect of orientation, another prominent feature is the decrease of conductivity with crystallinity X at low temperatures. This is best brought out by the data on PET, which have been measured[1] over a wide range of crystallinities and down to 1.5K (*Figure 8*). It is evident that boundary resistance between the crystalline and amorphous phases plays the dominant role at such temperature.

The maximal effect of boundary resistance is to completely block heat flow into the crystalline phase, this being equivalent to having a non-conducting crystalline phase. So if for the moment we assume, as in analysing the high temperature data, that the crystallites are spherical, then the limiting isotropic conductivity may be obtained from equation (13) by setting both $k_{\parallel}$ and $k_{\perp}$ to zero to give

$$K_i/K_a = 2(1 - X)/(2 + X) \qquad (21)$$

This limiting curve is shown by the dashed line in *Figure 8*. Since the data at the lowest temperature fall even faster with X than this limiting curve, we are forced to conclude that the low temperature data are not consistent with spherical crystallinities. This may at first seem somewhat puzzling in

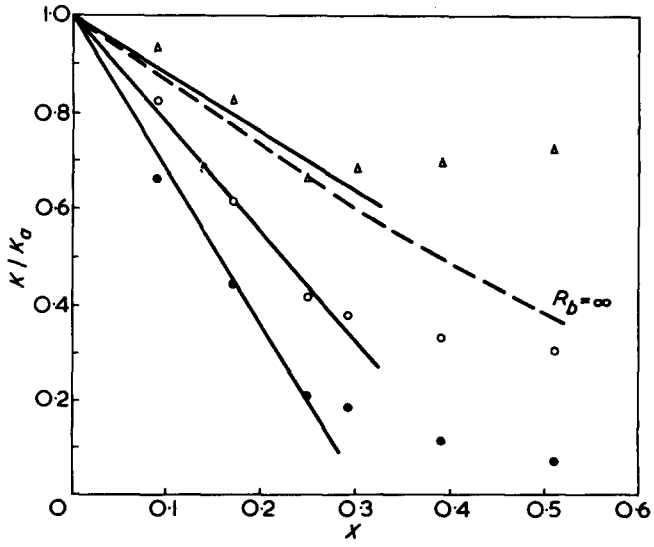

Figure 8 The ratio K/K_a for isotropic PET as functions of crystallinity. Data at 1.5K (●), 5K (○) and 10K (△) from ref 1. – – – –, is calculated using equation (21)

view of the success of the same assumption at high temperatures. However, bearing in mind that boundary resistance is expected to impede heat flow from the interlamellar amorphous region to both the crystalline and the intermosaic regions, it is clear that the basic unit for blocking heat flow consists ot a number of mosaic blocks. This situation can be roughly described by assigning to the basic units an aspect ratio γ (width/thickness) much larger than one.

For simplicity, we consider the crystalline phase as isotropic, with conductivity K_c. This is justified at low temperature because both $K_{c/\!/}$ and $K_{c\perp}$ are expected to be so much greater than K_a that their exact values are immaterial. The theoretical analysis for a dilute ($X \lesssim 0.2$) dispersion of isotropic inclusions with boundary resistance has been carried out[32] in the case of spheroidal inclusions, with axes $2a$, $2a$, $2b$ (so that $\gamma = a/b$), the result being:

$$\frac{K_i}{K_a} = 1 + X\beta \tag{22}$$

where

$$\beta = \frac{1}{3}(2\beta_x + \beta_z) \tag{23}$$

and

$$\beta_i = \frac{k - 1 - \dfrac{rkt_i}{1 - s_i}}{1 + (k-1)s_i + rkt_i} \simeq \frac{1 - \dfrac{rt_i}{1 - s_i}}{s_i + rt_i} \qquad i = x,z \tag{24}$$

the latter form being valid for $k \equiv K_c/K_a \gg 1$ as in the present case. The dimensionless parameter r is related to the boundary resistance R_b as:

$$r = K_a R_b (a^2 b)^{-1/3}$$

and the dependence of s_i, t_i on γ is given in ref 32.

Equation (22) predicts that, for small X, K_i/K_a is linear in X and this agrees with the data (*Figure 8*). By fitting the small X portion of the data, we have obtained the slope β for each temperature. Extrapolating these to $T = 0$ gives an asymptotic value of $\beta = -3.4$. This asymptotic value is important because as $T \to 0$, we expect $r \to \infty$, so equation (24) further reduces to:

$$\beta_i = \frac{-1}{1 - s_i}$$

Thus the asymptotic value of β depends only on the effective aspect ratio γ which is found to be 11.5.

With γ and thus s_i, t_i known, β at each temperature depends only on the parameter r, which can therefore be determined. It should be noted that r is X-independent, even though we have used the low X data to extract its value. Taking $2b \simeq 150$ Å to simulate a lamella thickness[33] of about 100 Å, and using the known K_a, we have calculated R_b for each temperature and plotted the results in *Figure 9*. We see that below about 6K R_b varies approximately as T^{-2} (this being independent of the value taken for b), a behaviour in agreement with that for other interfaces which have been directly measured[34,35]. It is to be noted that this temperature dependence disagrees with Little's theory[36], which predicts $R_b \propto T^{-3}$. Nevertheless, the value of R_b at 1.5K is within a factor of 2 of that calculated[1] from Little's theory.

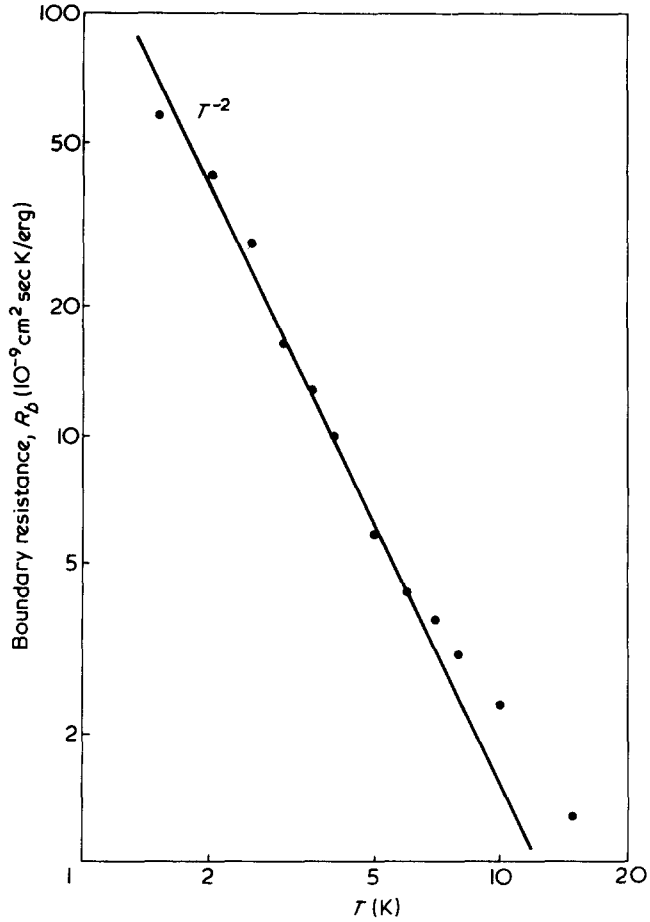

Figure 9 The boundary resistance between the amorphous and crystalline regions of PET as a function of temperature. R_b is obtained by fitting equation (22) to the experimental data

Another consequence of the interface boundary resistance is that, at sufficiently low temperatures, heat flow is largely excluded from the crystalline phase, so that the difference between $K_{c/\!/}$ and $K_{c\perp}$ becomes irrelevant. This leads to an absence of marked anisotropy at low temperatures, which is indeed the feature observed[2–4].

CONCLUSION

In this paper we have formulated a simple and realistic model for the thermal conductivity of semicrystalline polymers at high temperatures. The result has been successfully applied to a number of polymers (PET, PE, PP) and has reproduced both the crystallinity- and orientation- dependence. According to this model the thermal conductivity of a bulk sample is insensitive to the actual conductivity of the crystallites along the chain direction (since this is so large), but the conductivity normal to the chain direction has been extracted from the data. Its value and temperature dependence offer some clues as to the phonon-scattering mechanism in the crystalline phase of each polymer.

A recently proposed model for composite materials, which takes into account the boundary resistance between the two phases in a material, has been applied to the low temperature data for PET. The extreme simplicity of the theory in the low temperature limit allows a simple determination of the effective shape of the crystalline units res-

ponsible for obstructing heat flow. The T^{-2} behaviour of the boundary resistance found here, though in agreement with other experimental work, is inconsistent with Little's theory, which predicts a T^{-3} dependence. A further understanding of this discrepancy may shed some light on the mechanism of phonon scattering at the boundary between two phases.

ACKNOWLEDGEMENTS

We are grateful to Professor I. M. Ward, Dr D. Greig, Dr A. G. Gibson and Mr M. Sahota of the University of Leeds, and Dr H. G. Kilian and Dr M. Pietralla of Universität Ulm for sending their experimental data before publication. Thanks are also due to Mr F. K. Lau for drawing the Figures.

REFERENCES

1 Choy, C. L. and Greig, D. *J. Phys. (C)* 1975, **8**, 3121
2 Burgess, S. and Greig, D. *J. Phys. (C)* 1975, **8**, 1637
3 Choy, C. L. and Greig, D. *J. Phys. (C)* 1977, **10**, 169
4 Gibson, A. G., Grey, D., Sahota, M., Ward, I. M. and Choy, C. L. *J. Polym. Sci. (B)* in press
5 Hennig, J. and Knappe, W. *J. Polym. Sci. (C)* 1964, **6**, 167
6 Reese, W. *J. Appl. Phys.* 1966, **37**, 864
7 Geil, P. H. 'Polymer Single Crystals', Wiley, New York, 1963
8 Statton, W. D. *J. Polym. Sci. (C)* 1967, **18**, 33
9 Kavesh, S. and Schultz, J. M. *J. Polym. Sci. (A-2)* 1970, **8**, 243
10 Loboda-Čačković, J., Hosemann, R., Čačković, H., Ferrero, F. and Ferracini, E. *Polymer*, 1976, **17**, 303
11 Yeh, G. S. Y., Hosemann, R., Loboda-Čačković, J. and Čačković, H. *Polymer* 1976, **17**, 309
12 Takayanagi, M. and Kajiyama, T. *J. Macromol. Sci. (B)* 1973, **8**, 1
13 Maxwell, J. C. 'A Treatise on Electricity and Magnetism', Clarendon Press, Oxford, 1892, Vol. 1, p 435
14 Rayleigh, Lord. *Phil. Mag.* 1892, **34**, 481
15 Meredith, R. E. and Tobias, C. W. *J. Appl. Phys.* 1960, **31**, 1270
16 Jeffrey, D. J. *Proc. R. Soc. London (A)* 1973, **335**, 395
17 Eiermann, K. *Kolloid Z. Z. Polym.* 1964, **201**, 3
18 Ziman, J. M. 'Electrons and Phonons' Oxford University Press, London 1960
19 Eucken, A. and Schröder, E. *Ann. Phys.* 1939, **36**, 609
20 Hennig, J. *J. Polym. Sci. (C)* 1967, **16**, 2751
21 Müller, F. H. *J. Polym. Sci. (C)* 1967, **20**, 61
22 Knappe, W. *Adv. Polym. Sci.* 1970, **7**, 477
23 Lakkad, S. C., Miatt, B. B. and Parsons, B. *J. Phys. (D)* 1972, **5**, 1304
24 Killian, H. G. and Pietralla, M. *Polymer*, to be published
25 Ward, I. M. 'Mechanical Properties of Polymers', (Wiley-Interscience, New York, 1971
26 Hadley, D. W. and Ward, I. M. 'Structure and Properties of Oriented Polymers' (Ed. I. M. Ward), Applied Science Publishers, London, 1975, p 264
27 Hansen, D. and Bernier, G. A. *Polym. Eng. Sci.* 1972, **12**, 204
28 Dumbleton, J. H., Murayama, T. and Bell, J. P. *Kolloid Z. Z. Polym.* 1968, **228**, 54
29 Williams, T. *J. Mater. Sci.* 1973, **8**, 59
30 Gupta, V. B. and Ward, I. M. *J. Macromol. Sci. (B)* 1971, **5**, 629
31 Pietralla, M. *Kolloid Z. Z. Polym.* 1976, **254**, 249
32 Chen, F. C., Choy, C. L. and Young, K. *J. Phys. (D).* 1977, **10**, 57
33 Overton, J. R. and Haynes, S. K. *J. Polym. Sci. (C)* 1973, **43**, 9
34 Garret, K. W. and Rosenberg, H. M. *J. Phys. (D)* 1974, **7**, 1247
35 Schmidt, C. *Cryogenics* 1975, **15**, 17
36 Little, W. A., *Can. J. Phys.* 1959, **37**, 334
37 Knappe, W. and Lohe, P. *Kolloid Z. Z. Polym.* 1963, **189**, 114